OPTOELECTRONICS LETTERS Vol.10 No.4, 1 July 2014

# Wavelet-denoising technique in near-infrared methane detection based on tunable diode laser absorption spectroscopy*

**GAO Zong-li** (高宗丽)[1], **YE Wei-lin** (叶玮琳)[2], **ZHENG Chuan-tao** (郑传涛)[1]**, **and WANG Yi-ding** (王一丁)[1]**

*1. State Key Laboratory on Integrated Optoelectronics, College of Electronic Science and Engineering, Jilin University, Changchun 130012, China*

*2. College of Engineering, Shantou University, Shantou 515063, China*

(Received 8 April 2014)



A novel wavelet denoising (WD) assisted wavelength modulation technique is proposed for improving near-infrared detection performance on methane concentration based on tunable diode laser absorption spectroscopy (TDLAS). Due to the ability of multi-level analytical resolutions both in time- and frequency-domains, the noise contained in the differential signal is greatly suppressed. Sensor mechanical part, optical part and electrical part are integrated, and a portable detection device is finally developed. Theory and formulations of the WD-assisted wavelength modulation technique are presented, and experiments are carried out to prove the normal function on the extraction of the second harmonic (2*f*) signal from severely polluted differential signal by using the technique. By virtue of WD's suppression on noises, the sensing characteristics on $CH_4$ concentration are improved, and the limit of detection (LOD) is decreased from $4\times10^{-6}$ (without WD processing) to $10^{-6}$. The proposed technique can also be used for the measurement on the concentration of other gases with corresponding near-infrared distributed feedback lasers.

**Document code:** A **Article ID:** 1673-1905(2014)04-0299-5

**DOI** 10.1007/s11801-014-4057-z

For consideration of safe production in coal mine industrial environment, the research in the field of $CH_4$ detection[1-4] shows the same increasing trend as the detection on other trace gases, including NO, CO, $SO_2$, etc. Owning to the advantages, including wide measuring range, high sensitivity, good selectivity, longevity and fast response, the spectrum absorption becomes a well-known technique on $CH_4$ detection[5-7]. Tunable diode laser absorption spectroscopy (TDLAS) can overcome the above disadvantages and satisfy more difficult measurement requirements, and it has been widely used in infrared trace gas detection[8-11]. As a superior signal processing technique, wavelet denoising (WD)[12-14], which possesses multi-level analytical resolutions both in time- and frequency-domains, is an efficient tool to remove noises from severely polluted signal. In this paper, a $CH_4$ detection device based on WD-assisted wavelength modulation technique is experimentally demonstrated. By doing wavelet transformation on polluted differential signal between detection channel and reference channel, the expansion coefficients under different levels are obtained. The noises, whose expansion coefficients are different from those of the pure signal, can be removed through the self-adaptive multi-threshold WD method.

The configuration of the proposed $CH_4$ detection device is shown in Fig.1, which generally contains two parts. The optical part is configured with a gas-cell, a near infrared (NIR) TDL source and two NIR detectors. The electrical part is equipped with an electric board for driving, modulating and temperature-controlling of the TDL, dealing with sensing signals and performing data-processing, calculation and displaying. The generated laser beam is split into two beams with a fiber optical beam splitter (FOBS). The reference laser beam firstly propagates through an optical attenuator (OA), and then reaches the reference NIR-detector for generating the reference current $i_r$; the detection laser beam passes into the gas cell through a fiber collimator (FC), then propagates out of the gas cell through another FC, and finally the absorbed beam reaches the detection

* This work has been supported by the Science and Technology Council of China (No.2013BAK06B04), the National Natural Science Foundation of China (No.61307124), the Science and Technology Department of Jilin Province of China (No.20120707), the Technology Department of Changchun City of China (No.11GH01), the Foundation for Distinguished Young Talents in Higher Education of Guangdong (No.2013LYM_0030), the Research Award Fund for Outstanding Young Teachers of Shantou University (No.YR12005), and the Scientific Research Foundation Project of Shantou University (No.NTF12022).

** E-mails: zhengchuantao@jlu.edu.cn; wangyiding48@yahoo.com.cn

NIR-detector for generating the detection current $i_{\mathrm{d}}$. $i_{\mathrm{r}}$ and $i_{\mathrm{d}}$ are transformed to voltage signals through the bias circuits, denoted by $u_{\mathrm{r}}$ and $u_{\mathrm{d}}$. After subtraction and full-scale selection (FS-S), the differential signal $u_{\mathrm{d=}}=u_{\mathrm{r}}-u_{\mathrm{d}}$ is sampled by a 16-bit ADC and converted to digital signal.

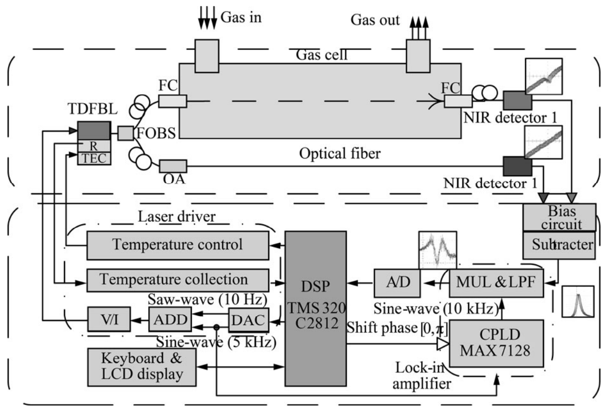


**Fig.1 Configuration of the proposed $CH_4$ detection device using WD-assisted wavelength modulation technique**

The scan and modulation signal used to drive the DFB laser is

$$u(t)=u_{\mathrm{saw}}(t)+u_{\cos}(t), \tag{1}$$

where $u_{\mathrm{saw}}(t)=(A_{\mathrm{jc}}/2)\left[1+2f_{\mathrm{jc}}\left(t-T_{\mathrm{jc}}/2\right)\right]$ , $u_{\cos}(t)=(A_{\cos}/2)\cos(\omega_{\cos}t)$ and $T_{\mathrm{jc}}=1/f_{\mathrm{jc}}$. Under the operation of $u(t)$, the emitting light intensity distribution over the 2-D plane and the absorption coefficient are

$$I(x,y,t)=nI_0\left[1+mu(t)\right]f(x,y), \tag{2}$$

$$\alpha(t)=\frac{\alpha_0}{1+\left[(\upsilon_0-\upsilon_{\mathrm{g}})/\gamma+\delta u(t)/\gamma\right]^2}, \tag{3}$$

where $f(x,y)$ is the 2-D normalized distribution function of light intensity, $I_0$ is the central emitting light intensity, $m$ is light modulation coefficient, $\upsilon_{\mathrm{g}}$ is central absorption wave-number, $\upsilon_0$ is central emitting light wave-number determined by the operation temperature of DFB laser, $\delta$ is light wavelength modulation coefficient, $\alpha_0=\dfrac{N_0 S}{\pi\gamma}$ is the light absorption coefficient at $\upsilon_0$, $S$ is the light absorption intensity at $\upsilon_0$, $\gamma$ is the half-width of the absorption peak at $\upsilon_0$, and $N_0$ is the Avogadro's constant.

Let gas concentration be $C$, and absorption path length be $L$. Considering residual amplitude modulation, for the detection channel, based on Beer-Lambert law, the radiation intensity distribution over the sensing plane $S_{\mathrm{D}}$ can be expressed as

$$I_{\mathrm{t}}(x,y,t)=nI_0 f(x,y)\left[1+mu(t)\right]\exp\left[-\alpha(t)CL\right]=$$
$$nI_0 f(x,y)\left[1+mu(t)\right]\left[1-\alpha(t)CL\right], \tag{4}$$

where $n$ is the attenuation coefficient of OA, and $\alpha(\upsilon,t)$ is the absorption coefficient dependent on the emitting wavelength of DFB laser. The emitting light is simply regarded to be perpendicular with the sensing plane, and the total radiation intensity to detector #1 is

$$\psi_{\mathrm{t}}(\upsilon,t)=nI_0\left(\iint_{S_{\mathrm{D}}}f(x,y)\mathrm{d}x\mathrm{d}y\right)\times$$
$$\left[1+mu(t)\right]\left[1-\alpha(\upsilon,t)CL\right]. \tag{5}$$

For the reference channel, the total radiation intensity reaching detector #2 is

$$\psi_{\mathrm{r}}(\upsilon,t)=(1-n)I_0\left(\iint_{S_{\mathrm{D}}}f(x,y)\mathrm{d}x\mathrm{d}y\right)\left[1+mu(t)\right]. \tag{6}$$

Let $G=\iint_{S_{\mathrm{D}}}f(x,y)\mathrm{d}x\mathrm{d}y$. After optical-to-electrical conversion and being amplified, the two signals will be modified to

$$u_{\mathrm{t}}(t)=K_{\mathrm{t}}D_{\mathrm{oe}}^{\mathrm{t}}GnI_0\left[1+mu(t)\right]\left[1-\alpha(\upsilon,t)CL\right], \tag{7}$$

$$u_{\mathrm{r}}(t)=K_{\mathrm{r}}D_{\mathrm{oe}}^{\mathrm{r}}G(1-n)I_0\left[1+mu(t)\right], \tag{8}$$

where $K_{\mathrm{t}}$ and $D_{\mathrm{oe}}^{\mathrm{t}}$ are the amplifying factor and optical-to-electrical conversion coefficient for the detection-channel, respectively, and $K_{\mathrm{r}}$ and $D_{\mathrm{oe}}^{\mathrm{r}}$ are those for the reference-channel, respectively. The differential signal between $u_{\mathrm{t}}$ and $u_{\mathrm{r}}$ is

$$u_{\mathrm{r}}(t)-u_{\mathrm{t}}(t)=I_0[1+mu(t)][K_{\mathrm{r}}D_{\mathrm{oc}}^{\mathrm{r}}G(1-n)-$$
$$K_{\mathrm{t}}D_{\mathrm{OC}}^{\mathrm{t}}Gn+K_{\mathrm{t}}D_{\mathrm{OC}}^{\mathrm{t}}Gn\alpha(t)CL]. \tag{9}$$

Tuning the attenuation coefficient $n$, we have $K_{\mathrm{r}}D_{\mathrm{oe}}^{\mathrm{r}}G\times(1-n)-K_{\mathrm{t}}D_{\mathrm{oe}}^{\mathrm{t}}Gn=0$. With the satisfaction of $mu(t)<<1$, Eq.(11) will be changed to

$$u_{=}(t)=u_{\mathrm{r}}(t)-u_{\mathrm{t}}(t)=K_{\mathrm{t}}D_{\mathrm{oe}}^{\mathrm{t}}Gn\alpha(t)CL. \tag{10}$$

By using an ADC, the analogue signal $u_{=}(t)$ is converted to discrete digital signal $u_{\mathrm{d=}}(k)$ as

$$u_{\mathrm{d=}}(k)=K_{\mathrm{t}}D_{\mathrm{oe}}^{\mathrm{t}}Gna(kT_{\mathrm{s}})CL, \tag{11}$$

where $T_{\mathrm{s}}$ is sampling period.

Considering the noises and interferences (defined by $n(k)$ ) introduced by electric circuits, the signal should be expressed as

$$u'_{\mathrm{d=}}(k)=u_{\mathrm{d=}}(k)+n(k). \tag{12}$$

With Fourier transformation, the second harmonic (2$f$) signal can be achieved by the following numerical integral

$$S_{2f}\left(k\right)=\sum_{n=k-N_{\mathrm{num}}}^{k}\left[u'_{\mathrm{d=}}\left(n\right)\cos\left(2\omega_{\cos}nT_{\mathrm{s}}\right)\right]. \quad (13)$$

Without WD processing, the differential signal contains too many noises, as shown by the lower trace in Fig.2, and the extracted 2*f* signal reveals fluctuation, as shown by the upper trace in Fig.2. The situation becomes even worse when the concentration gets further lower. This will deteriorate the detection performance. Therefore, as an innovation of this paper, inside the DSP, the sampled differential signal is firstly digitally processed with WD, namely

$$u''_{\mathrm{d=}}\left(k\right)=\mathrm{WD}\left[u'_{\mathrm{d=}}\left(k\right)\right]. \quad (14)$$

Then, Eq.(13) is used to extract the 2*f* signal.

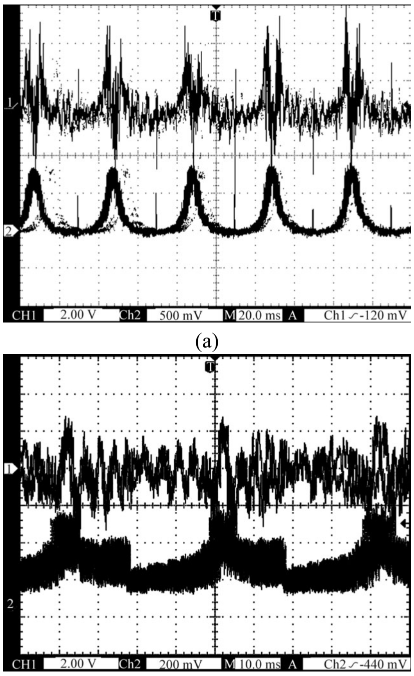


**Fig.2 Observed waveforms of the differential signal and 2*f* signal under (a) 1% concentration and (b) 0.05% concentration**

The wavelet denoising principle is described below. Let $\varphi_{jk}(t)=2^{-j/2}\varphi(2^{-j}t-k)$ be the sub-wavelet function obtained by the transformation on the mother wavelet function $\varphi(t)$, and let $h(n)$ and $g(n)$, $n=0,\ 2,\ \cdots,N-1$, be the high-pass and low-pass weighting coefficients of $\varphi(t)$. For the discrete differential signal $c_n^0=u_{\mathrm{d=}}\left(n\right),n=0,\ 2,\ \cdots,M-1$, the *j*-th discrete wavelet transformation (DWT) on *u* ( $c_n^j$ and $d_n^j$, $j=0,1,\cdots,J-1$ ) can be regarded as the expansion on the (*j*-1)-th discrete wavelet transformation (DWT) on *u* ( $c_n^{j-1}$ ), which is written as

$$c_k^{j+1}=\sum_{n\in Z}h\left(n\right)c_{2k+n}^{j}, \quad (15)$$

$$d_k^{j+1}=\sum_{n\in Z}g\left(n\right)c_{2k+n}^{j}. \quad (16)$$

For the *j*-th deposition, define the lengths of $\boldsymbol{c}^j$, $\boldsymbol{d}^j$, $\boldsymbol{d}^{j-1}$, $\cdots$, $\boldsymbol{d}^1$ as $k_{j,\max}$, $k_{j,\max}$, $k_{j-1,\max}$, $\cdots$, $k_{1,\max}$.

Before recovering the original data using inversion DWT (IDWT), the expansion coefficients should be processed for the suppression on contained noises. Because the frequent components of $u_{\mathrm{d=}}\left(n\right)$ are complicated, the denoising is carried out considering the coefficient correlations both inside the same deposition scale and between different deposition scales. The included WD steps are below.

(1) Given a parameter $\varsigma$, calculate the coefficient $\lambda=\dfrac{\sqrt{2\ln M}}{\varsigma k_{1,\max}}\sum_{k=0}^{k_{1,\max}-1}d_k^1$.

(2) At the *j*-th wavelet deposition scale, define the weighting coefficient vector as $\boldsymbol{w}_j=\left[\boldsymbol{c}^j,\boldsymbol{d}^j,\boldsymbol{d}^{j-1},\cdots\boldsymbol{d}^1\right]$, and construct a coefficient matrix as $\boldsymbol{W}=\left[\boldsymbol{w}_1,0,\cdots,0;\boldsymbol{w}_2,0,\cdots,0;\cdots\boldsymbol{w}_J\right]^{\mathrm{T}}$. Note that, the length of $\boldsymbol{w}_j$ is shorter than that of $\boldsymbol{w}_{j+1}$, so '0' elements are supplemented to make the length of each sub-vector of the matrix be equal.

(3) Determine the matrix ***nn***, whose elements are $nn_{j,k}=\begin{cases}\sqrt{W_{j,1}^2+W_{j,2}^2},k=1\\ \sqrt{W_{j,k-1}^2+W_{j,k}^2+W_{j,k+1}^2},1<k<k_{J,\max}\\ \sqrt{W_{j,k_{J,\max}-1}^2+W_{j,k_{J,\max}}^2},k=k_{J,\max}\end{cases}$. Calculate the binaration matrix ***ii***, whose elements are $ii_{j,k}=\begin{cases}1,nn_{j,k}^2>\lambda^2,W_{j,k}\dfrac{1-\lambda^2}{nn_{j,k}^2}\neq 0\\ 0,\mathrm{otherwise}\end{cases}$, and calculate the differential matrix ***ee*** based on ***ii***, whose elements are $ee_{j,k}=\begin{cases}ee_{j,k},k=1\\ ee_{j,k}-ee_{j,k-1},\mathrm{otherwise}\end{cases}$.

(4) Obtain the index matrices ***aa*** and ***bb***, whose elements satisfy $aa_{j,m}=k\big|_{ee_{j,k}=1}$ and $bb_{j,m}=k\big|_{ee_{j,k}=-1}$.

(5) Determine the horizontal correlation matrix ***hh*** inside the same deposition scale, whose elements are $hh_{j,k}=\begin{cases}bb_{j,m}-aa_{j,m},k>aa_{j,m}\text{ and }k<bb_{j,m}\\ 0,\mathrm{otherwise}\end{cases}$. Determine the vertical correlation matrix ***vv*** between different deposition scales, whose elements are $vv_{j,k}=\begin{cases}ii_{j,k}\times ii_{j+1,k},j<J\\ ii_{j,k},j=J\end{cases}$.

(6) Determine the decision coefficient matrix ***dd*** considering horizontal and vertical coefficients, and its elements are $dd_{j,k}=\begin{cases}1,vv_{j,k}=1\text{ or }hh_{j,k}>h_{\mathrm{thr}}\\ 0,\mathrm{otherwise}\end{cases}$, where $h_{\mathrm{thr}}$ is the threshold value of the horizontal correlation element, which is set to be an integer within 3-7.

(7) Calculate the new wavelet deposition coefficient matrix $\tilde{\boldsymbol{W}}$, whose elements are $\tilde{W}_{i,j}=W_{i,j}\times dd_{i,j}$.

(8) For the *j*-th deposition, $\tilde{c}_k^j=\tilde{W}_{j,k}$, $\tilde{d}_k^j=\tilde{W}_{j,k+k_{j,\max}}$,

$\tilde{d}_k^{j-1} = \tilde{W}_{j-1,k+\sum_{v=j}^{j-2} k_{v,\max}}$, …, $\tilde{d}_k^{1} = \tilde{W}_{j-1,k+\sum_{v=j}^{2} k_{v,\max}}$. Then recover the original data $c_k^0$ by performing $c_k^{j-1} = \sum_k \tilde{c}_k^j h_{n-2k} + \sum_k \tilde{d}_k^j g_{n-2k}$ for $j$ interactions. Denote $c_k^0$ obtained from the $j$-th wavelet construction as $c_k^{j,0}$.

(9) An average value is finally adopted to evaluate the original data as $\tilde{u}_{d,=}(k) = \tilde{c}_k^0 = \frac{1}{J}\sum_{j=1}^{J} \tilde{c}_k^{j,0}$.

Experiments are carried out to verify the proposed WD method. The differential signal is sampled, and the sampled dot number per period is $M$=20 000. C-language-based WD program using CCS 3.0 platform is compiled for the DSP. The selected mother-wavelet function is 'db9' and the wavelet deposition scale is $J$=4. The data of the differential signal, denoised signal and the extracted 2$f$ signal are sent to a computer via UART communication port for data storage and observation.

For the sub measurement scale of 0—$10^{-3}$, Fig.3 shows the WD processing results on the measured differential signals under the concentrations of $10^{-5}$, $5\times10^{-6}$, $2\times10^{-6}$ and $10^{-6}$, respectively. It can be found that after WD processing, the noises are sufficiently suppressed. In Figs.3(a) and (b), the fluctuations of the two 2$f$ signals almost disappear compared with those without using WD, and this will be helpful for enhancing detection stability. In Figs.3(c) and (d), before WD processing, the 2$f$ signals cannot be extracted; however, after WD processing, the waveforms of the two 2$f$ signals are well observed with small noises, and this will be helpful for improving the MDL and sensitivity.

The limit of detection (LOD) and sensitivity under the situations of using WD and without using WD are mainly dependent on the noise levels under the two cases. At an initial concentration, the detection sensitivity can be regarded as the minimum $CH_4$ concentration change producing a variation in the amplitude of 2$f$ signal which can be obviously recognized by the system. Experiment was done below. The gas sample with an initial concentration was firstly prepared; then the concentration was slightly modified by injecting a proper amount of pure $CH_4$ until the minimum detection amplitude was steadily lower than the maximum detection amplitude under the initial concentration. Note that, after each $CH_4$ injection, 30 detections on the amplitude of the 2$f$ signal were conducted. Under extremely low concentration range, Fig.4 shows the detected amplitude of the 2$f$ signal within 0—$10^{-5}$, where the concentration is slightly increased by $10^{-6}$. We can find from Fig.4(b) that when WD is unused, the variation ranges of the detected amplitude under 0, $10^{-6}$, $2\times10^{-6}$ and $3\times10^{-6}$ are overlapped with each other because of noises, and as the concentration increases to $4\times10^{-6}$, the minimum detected amplitude begins to be larger than the maximum detected amplitude under 0. Thus the MDL in this case is about $4\times10^{-6}$. When WD is used (Fig.4(a)), because the noise level is minimized, the MDL is improved to about $10^{-6}$. Additionally, within this range, the detection sensitivity is decided to be about $2\times10^{-6}$ under both two cases.

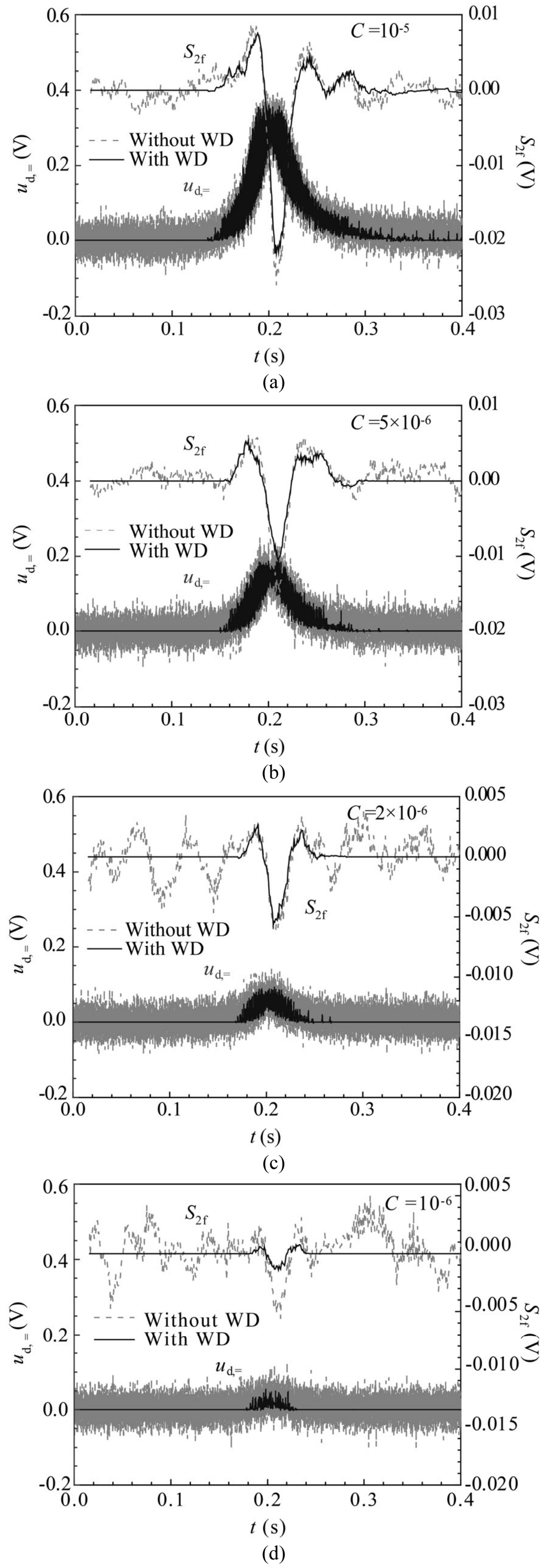


**Fig.3 For the sub measurement scale of 0—$10^{-3}$, the measured differential signals and the extracted 2$f$ signals under the concentrations of (a) $10^{-5}$, (b) $5\times10^{-6}$, (c) $2\times10^{-6}$, and (d) $10^{-6}$, respectively**

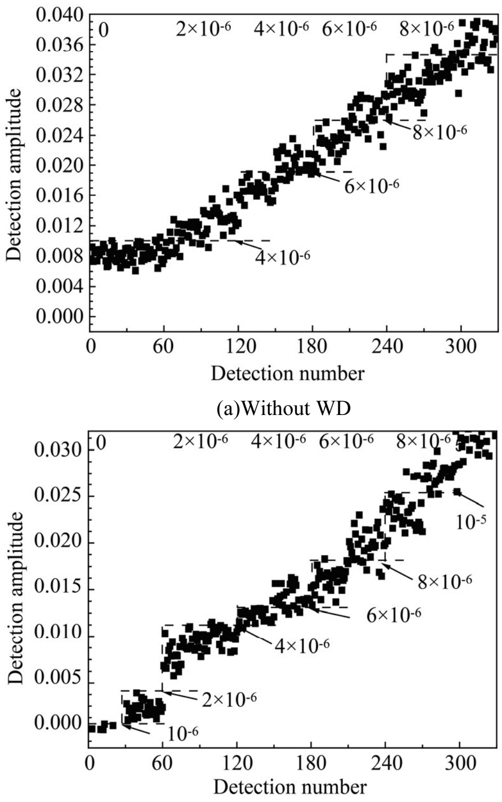


(a)Without WD

(b) With WD

**Fig.4 The detected amplitudes of the 2*f* signals within 0—$10^{-5}$ concentration under the cases of (a) using WD and (b) without using WD, where 30 detections are performed for one gas sample**

As a conclusion, a novel WD-assisted wavelength modulation technique is proposed for improving detection performance on methane concentration based on TDLAS, and due to the ability of multi-level analytical resolutions both in time- and frequency-domains, the noise contained in the differential signal is greatly suppressed. Experiments are carried out to prove the normal function on the extraction of 2*f* signal from severely polluted differential signal using the proposed technique. By virtue of WD's suppression on noises, the sensing characteristics on $CH_4$ concentration are improved through experiment.

## References


[1] S. L. Bai, L. Y. Chen, P. C. Yang, R. X. Luo, A. F. Chen and C. L. Chung, Sensors and Actuators B: Chemical **135**, 1 (2008).

[2] A. Kock, A. Tischner, T. Maier, M. Kast, C. Edtmaier, C. Gspan and G. Kothleitner, Sensors and Actuators B: Chemical **138**, 160 (2009).

[3] Y. Zhang, W. Gao, Z. Song, Y. An, L. Li, Z. Song, W. W. Yu and Y. D. Wang, Sensors and Actuators B: Chemical **147**, 5 (2010).

[4] J. Liu, Q. Tan, W. Zhang, C. Xue, T. Guo and J. Xiong, Measurement **44**, 823 (2011).

[5] U. Willer, M. Saraji and A. Khorsandi, Optics and Lasers in Engineering **44**, 699 (2006).

[6] A. Zybin, J. Koch and D. J. Butcher, Journal of Chromatography A **1050**, 35 (2004).

[7] G. J. Zhang and X. L. Wu, Optics and Lasers in Engineering **42**, 219 (2004).

[8] Z. Peng, Y. Ding, L. Che, X. Li and K. Zheng, Optics Express **19**, 23104 (2011).

[9] Philip A. Martin, Chem. Soc. Rev. **31**, 201 (2002).

[10] G. Durry, J. S. Li, I. Vinogradov, A. Titov, L. Joly, J. Cousin, T. Decarpenterie, N. Amarouche, X. Liu, B. Parvitte, O. Korablev, M. Gerasimov and V. Zéninari, Appl. Phys. B: Lasers and Opt. **99**, 339 (2010).

[11] Q. Tana, W. Zhang, C. Xue, J. Xiong, Y. Ma and F. Wen, Optics & Laser Technology **40**, 703 (2008).

[12] A. Khare, U. S. Tiwary, W. Pedrycz and M. Jeon, Imaging Science J. **58**, 340 (2010).

[13] P. Gorgel, A. Sertbas and O. N. Ucan, J. Medical Systems **34**, 993 (2010).

[14] S. Gupta, R. C. Chauhan and S. C. Saxena, J. Med. Eng. Technol. **29**, 208 (2005).